



CHORUS

This is the accepted manuscript made available via CHORUS. The article has been published as:

Fluctuations of the gluon distribution from the small- x effective action

Adrian Dumitru and Vladimir Skokov

Phys. Rev. D **96**, 056029 — Published 29 September 2017

DOI: [10.1103/PhysRevD.96.056029](https://doi.org/10.1103/PhysRevD.96.056029)

Fluctuations of the gluon distribution from the small- x effective action

Adrian Dumitru

*Department of Natural Sciences, Baruch College, CUNY,
17 Lexington Avenue, New York, NY 10010, USA and*

The Graduate School and University Center, The City University of New York, 365 Fifth Avenue, New York, NY 10016, USA

Vladimir Skokov

RIKEN/BNL Research Center, Brookhaven National Laboratory, Upton, NY 11973, USA

The computation of observables in high energy QCD involves an average over stochastic semi-classical small- x gluon fields. The weight of various configurations is determined by the effective action. We introduce a method to study fluctuations of observables, functionals of the small- x fields, which does not explicitly involve dipoles. We integrate out those fluctuations of the semi-classical gluon field under which a given observable is invariant. Thereby we obtain the effective potential for that observable describing its fluctuations about the average. We determine explicitly the effective potential for the covariant gauge gluon distribution both for the McLerran-Venugopalan (MV) model and for a (non-local) Gaussian approximation for the small- x effective action. This provides insight into the correlation of fluctuations of the number of hard gluons versus their typical transverse momentum. We find that the spectral shape of the fluctuations of the gluon distribution is fundamentally different in the MV model, where there is a pile-up of gluons near the saturation scale, versus the solution of the small- x JIMWLK renormalization group, which generates essentially scale invariant fluctuations above the absorptive boundary set by the saturation scale.

I. INTRODUCTION

High-energy scattering in QCD at fixed transverse momentum scales probes strong color fields, i.e. the regime of high gluon densities [1]. In the high-energy limit physical observables, such as the forward scattering amplitude of a dipole from a hadron or nucleus, are typically expressed in terms of expectation values of various Wilson line operators O ; see, for example, Ref. [2]. The expectation value $\langle O \rangle$ corresponds to a statistical average¹ over the distribution of “small- x gluon fields”. For example, if quantum corrections are neglected this distribution is commonly described by the McLerran-Venugopalan (MV) model [4]:

$$\begin{aligned} -\nabla_{\perp}^2 A^+(x^-, x_{\perp}) &= g\rho(x^-, x_{\perp}), \\ Z &= \int \mathcal{D}\rho e^{-S[\rho]}, \quad S[\rho] = \int dx^- d^2x_{\perp} \frac{\text{tr} \rho(x^-, x_{\perp}) \rho(x^-, x_{\perp})}{2\mu^2(x^-)}. \end{aligned} \quad (1) \quad (2)$$

Here, A^+ is the covariant gauge *classical* field (describing the small- x gluon fields) sourced by the random valence charge density ρ which one averages over. $\int dx^- \mu^2(x^-)$ corresponds to the average color charge density squared per unit transverse area and is the only parameter of the model; it is proportional to the thickness of the nucleus $\sim A^{1/3}$. The expectation value of an electric Wilson line $V(x_{\perp})$, for example, is then computed as²

$$\langle \text{tr} V(x_{\perp}) \rangle = \frac{1}{Z} \int \mathcal{D}\rho e^{-S[\rho]} \text{tr} \mathcal{P} e^{-ig \int_{-\infty}^{\infty} dx^- A^+(x^-, x_{\perp})}. \quad (3)$$

The forward scattering amplitude $\mathcal{N}(r)$ of a quark - antiquark dipole of size $r = |y_{\perp} - x_{\perp}|$ is given by

$$\mathcal{N}(r) = \left\langle 1 - \frac{1}{N_c} \text{tr} V^{\dagger}(x_{\perp}) V(y_{\perp}) \right\rangle = \frac{1}{Z} \int \mathcal{D}\rho e^{-S[\rho]} \left[1 - \frac{1}{N_c} \text{tr} \mathcal{P} e^{ig \int_{-\infty}^{\infty} dx^- A^+(x^-, x_{\perp})} \mathcal{P} e^{-ig \int_{-\infty}^{\infty} dx^- A^+(x^-, y_{\perp})} \right]. \quad (4)$$

We employ hermitian generators. The size r where $\mathcal{N}(r)$ grows to order 1 defines the (inverse) saturation scale Q_s^{-1} . In the MV model one finds that $Q_s^2 \sim C_F g^4 \int dx^- \mu^2(x^-)$. For transverse momenta $q^2 \gg Q_s^2$ the Fourier transform of

¹ Kovner describes this as an average over the Hilbert space of the target, i.e. that the weight $W[A^+] \equiv \exp(-S[A^+])$ which determines the probability for a given configuration of A^+ is analogous to the modulus squared of the wave function of the target [3].

² $\log \langle \text{tr} V \rangle$ is power divergent in the IR and so requires a cutoff. We simply write the formal Eq. (3) to illustrate the averaging procedure. The dipole probe from Eq. (4) does not exhibit such a power-law divergence in the IR.

the forward scattering amplitude defines the dipole unintegrated gluon distribution

$$xG(x, q^2) \simeq g^2 \langle \text{tr} |A^+(q)|^2 \rangle. \quad (5)$$

Quantum corrections to the MV model modify the statistical weight $W[\rho] \equiv \exp(-S[\rho])$. Ref. [5] proposed a Gaussian “mean-field” approximation for $W[\rho]$ at small light-cone momentum fractions (far from the valence sources) which reproduces the proper gluon distribution (or dipole scattering amplitude) both at small ($q^2 \ll Q_s^2$) as well as at high ($q^2 \gg Q_s^2$) transverse momentum:

$$W_G[\rho] = e^{-S_G[\rho]}, \quad S_G[\rho] = \int d^2x_\perp d^2y_\perp \frac{\text{tr} \rho(x_\perp) \rho(y_\perp)}{\mu^2(x_\perp - y_\perp)}. \quad (6)$$

This non-local Gaussian can be rewritten in q -space as³

$$\begin{aligned} S_G[\rho] &= \int \frac{d^2q}{(2\pi)^2} \text{tr} \rho(q) \rho(-q) \int d^2r \frac{e^{-iqr}}{\mu^2(r)} \\ &\equiv \int \frac{d^2q}{(2\pi)^2} \frac{\text{tr} \rho(q) \rho(-q)}{\mu^2(q^2)}. \end{aligned} \quad (7)$$

This action reproduces the correct dipole scattering amplitude and Weizsäcker-Williams gluon distribution in the short distance (high transverse momentum) limit, c.f. ref [5], with

$$\mu^2(q^2) \simeq \mu_0^2 \left(\frac{q^2}{Q_s^2} \right)^{1-\gamma}. \quad (8)$$

Here, $\gamma \simeq 0.64$ is the BFKL anomalous dimension [6] (in the presence of a saturation boundary [7]). Q_s^2 and μ_0^2 are evaluated at the rapidity of interest (like in the MV model μ_0^2 is again proportional to the thickness of the nucleus $\sim A^{1/3}$). We will not spell out this dependence on Y explicitly since our focus here is not on the growth of Q_s with Y which is well known. For the present purposes the most important effect of the resummation of quantum fluctuations is that $\mu^2(q^2)$ increases with transverse momentum when $q^2 > Q_s^2$.

The paper is organized as follows. In Sec. II we present the basic idea for computing an effective potential for a given observable by introducing a constraint into the functional integral. In Sec. III, in order to illustrate the approach with a simple example we compute the effective potential for the number $\text{tr} \rho^2$ in the MV model on a single site. We then compute the effective potential for the covariant gauge gluon distribution function in Sec. IV. We proceed to calculate the fluctuations of the gluon multiplicity and of the average squared transverse momentum in Sec. V. In Sec. VI we present results of numerical Monte-Carlo simulations within the MV model and for the solution of the JIMWLK renormalization group equation. We end with a discussion and outlook in Sec. VII.

II. THE BASIC IDEA: INTRODUCING THE CONSTRAINT EFFECTIVE POTENTIAL

Expectation values such as those written in Eqs. (3,4) refer to a statistical average of an observable $O[\rho]$ over *all* configurations $\rho(x^-, x_\perp)$ from the ensemble $W[\rho]$. On the other hand, we may be interested in the value of an observable for a specific subset of configurations such as configurations with a high number of gluons or with a specific unintegrated gluon distribution. These represent more “global” measures averaging over all fluctuations of $\rho(x^-, x_\perp)$ which do not affect, say, the unintegrated gluon distribution. In other words, our goal is to perform the integral over ρ subject to the constraint that, for example, $O[A^+] = g^2 \text{tr} |A^+(q)|^2$ is fixed, thereby decomposing the space of all $\rho(q)$, or $A^+(q)$, into invariant subspaces (w.r.t. the given observable).

We illustrate the fluctuations of the gluon distribution originating from the fluctuations of the classical valence color charge density ρ in Fig. 1. For simplicity we show a simple example corresponding to the fluctuations of the color charge representation of a system composed of a quark and an anti-quark. The MV model describes the fluctuations of a system of many valence charges in a high-dimensional representation about the most likely representation [8, 9].

³ Note that we define $1/\mu^2(q^2) \equiv \int d^2r e^{-iqr} / \mu^2(r)$.

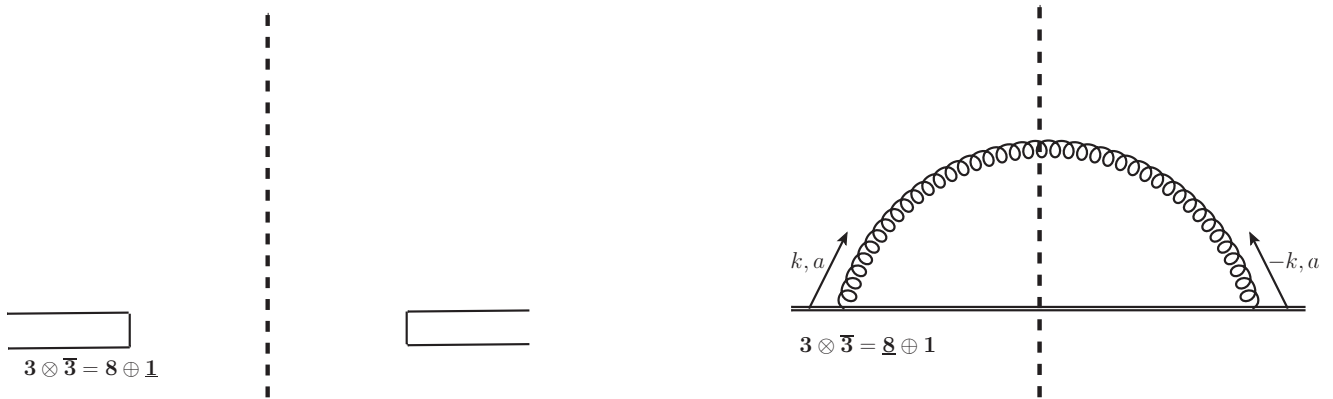


FIG. 1: Illustration of the fluctuation of the gluon distribution $g^2 \text{tr} A^+(k) A^+(-k)$ of a system of a quark and an anti-quark. The gluon couples coherently to the charges. Left: if the $q\bar{q}$ system is in the color singlet state there is no coupling to the field and the gluon distribution vanishes. Right: the octet representation has a non-vanishing gluon distribution.

The logarithm of the inverse of the partition function obtained after integrating out the orthogonal fluctuations of ρ then defines an effective potential⁴ for $O[\rho(q)] = g^2 \text{tr} |A^+(q)|^2$:

$$Z = \int \mathcal{D}X(q) e^{-V_{\text{eff}}[X(q)]}, \quad (9)$$

$$e^{-V_{\text{eff}}[X(q)]} = \int \mathcal{D}\rho(q) W[\rho(q)] \delta(X(q) - O[\rho(q)]). \quad (10)$$

The stationary point of $V_{\text{eff}}[X]$ corresponds to the extremal gluon distribution $X_s(q)$. In the limit of an infinite number of degrees of freedom, i.e. the large- N_c limit in our case⁵, $X_s(q)$ of course is equal to the expectation value of $\langle g^2 \text{tr} |A^+(q)|^2 \rangle$. Away from the stationary solution, the potential $V_{\text{eff}}[X]$ provides insight into the form of fluctuations about the extremum. Specifically, we shall analyze the correlation of fluctuations of the number of gluons (above the saturation scale) and their typical transverse momentum.

Fluctuations of various observables induced by the fluctuations of $\rho(x_\perp)$ have been analyzed before. For example, the multiplicity distribution of gluons with transverse momenta above Q_s [10] and the fluctuations of the real and imaginary parts of spatial Wilson loops [11] in the central region of a collision of two sheets of color charge have been analyzed. Angular harmonics of the dipole scattering amplitude $\mathcal{N}(r)$ for random individual configurations $\rho(x_\perp)$ of the target have been shown in Ref. [12] (the ensemble average is, of course, isotropic). The evolution of the imaginary part of the dipole S -matrix, i.e. of the odderon $O[A^+] = (-i/2N_c) \text{tr} [V_x V_y^\dagger - h.c.]$, has been discussed in Ref. [13]. Here, we describe how one can explicitly integrate out the fluctuations of ρ or A^+ under which a given observable is invariant in order to derive an effective potential for the observable itself. We apply our method specifically to compute the effective potential for the covariant gauge gluon distribution $\text{tr} |A^+(q)|^2$ from which we deduce the correlation of fluctuations of the multiplicity of hard gluons and of their typical transverse momentum. A somewhat similar procedure was previously used to compute the density matrix of the soft gluon fields and the associated entanglement entropy, see Ref. [14].

III. WARM-UP: EFFECTIVE POTENTIAL FOR $\text{tr} \rho^2$

We begin with the effective potential for $\text{tr} \rho^2$ on a single site. The procedure is essentially identical to that used in sec. III of Ref. [15] to compute the effective potential for Polyakov loops in a single-site matrix model.

⁴ More generally, this would give the effective action for the field $g^2 \text{tr} |A^+(q)|^2$.

⁵ To go beyond the large- N_c limit one would have to actually compute the integral over $X(q)$ in Eq. (9) which can be done by means of a Legendre transformation.

The partition function for a single site is

$$Z = \int \left(\prod_a d\rho^a \right) e^{-\text{tr} \rho^2 / \mu^2} . \quad (11)$$

$\rho \equiv \rho^a t^a$ denotes the random color charge density at the site and is an element of the algebra of the color group in the fundamental representation: $\text{tr} t^a t^b = \frac{1}{2} \delta^{ab}$. We shall keep only contributions to $V_{\text{eff}}(X)$ of order N_c^2 and drop terms of order 1.

The goal is to write (11) in the form

$$Z = \int dX e^{-V_{\text{eff}}(X)} , \quad X \equiv \text{tr} \rho^2 = \frac{1}{2} \rho^a \rho^a , \quad (12)$$

where $V_{\text{eff}}(X)$ is the effective potential for $\text{tr} \rho^2$. In other words, $e^{-V_{\text{eff}}(X)}$ is the partition sum for N_c^2 scalars ρ^a satisfying the constraint $\rho^a \rho^a = 2X$.

To compute $V_{\text{eff}}(X)$ we introduce a δ -function constraint in Eq. (11),

$$\begin{aligned} Z &= \int d\lambda \int \left(\prod_a d\rho^a \right) e^{-\text{tr} \rho^2 / \mu^2} \delta(\lambda - \text{tr} \rho^2) \\ &= \int d\lambda \int \frac{d\omega}{2\pi} e^{-\frac{\lambda}{\mu^2} - i\omega\lambda} \underbrace{\int \left(\prod_a d\rho^a \right) e^{i\omega \text{tr} \rho^2}}_{\tilde{Z}(\omega)} . \end{aligned} \quad (13)$$

The integral for $\tilde{Z}(\omega)$ is easily computed in spherical coordinates,

$$\begin{aligned} \tilde{Z}(\omega) &= \int dX \int \left(\prod_a d\rho^a \right) \delta\left(X - \frac{1}{2} \rho^b \rho^b\right) e^{\frac{1}{2} i\omega \rho^c \rho^c} \\ &\sim \int dX e^{i\omega X + \frac{1}{2} N_c^2 \log X} . \end{aligned} \quad (14)$$

In the last step we have dropped an irrelevant ω -independent normalization factor. This expression for $\tilde{Z}(\omega)$ then leads to

$$Z = \int dX e^{-\frac{X}{\mu^2} + \frac{1}{2} N_c^2 \log X} . \quad (15)$$

Hence, the effective potential is given by

$$V_{\text{eff}}(X) = \frac{X}{\mu^2} - \frac{1}{2} N_c^2 \log X . \quad (16)$$

The stationary point of this potential is

$$X_s \equiv \langle \text{tr} \rho^2 \rangle = \frac{1}{2} N_c^2 \mu^2 . \quad (17)$$

Of course, this result can be obtained directly from the correlator $\langle \rho^a \rho^b \rangle = \delta^{ab} \mu^2$ which follows from the action in Eq. (11).

IV. EFFECTIVE POTENTIAL FOR THE GLUON DISTRIBUTION

In this section we compute the effective potential for the gluon distribution $\text{tr} |A^+(q)|^2$ obtained from the field in covariant gauge. We will also comment briefly on the potential for the gluon distribution obtained from the light-cone gauge field $\text{tr} |A^i(q)|^2$.

It is convenient to work directly in momentum space. The partition function of the Gaussian model is taken as

$$Z = \int \left(\prod_q \prod_a d\rho_q^a \right) e^{-S[\rho]} , \quad S[\rho] = \int \frac{d^2 q}{(2\pi)^2} \frac{\text{tr} |\rho_q|^2}{\mu^2(q)} . \quad (18)$$

The constraint $(\rho_q)^* = \rho_{-q}$ is implicit. In general, $\mu^2(q)$ may depend on the transverse momentum which would correspond to a non-local Gaussian action in coordinate space; this dependence is also left implicit from now on since it is not essential for the following steps.

Our goal is to obtain an expression of the form

$$Z = \int \mathcal{D}X(q) e^{-V_{\text{eff}}[X(q)]} \quad (19)$$

for

$$X(q) \equiv g^2 \text{tr} |A^+(q)|^2 = \int d^2b d^2r e^{-iq \cdot r} g^2 \text{tr} A^+(x_\perp) A^+(y_\perp), \quad (20)$$

where $b = (x_\perp + y_\perp)/2$ and $r = y_\perp - x_\perp$. Since $A^+(q) = (g/q^2) \rho(q)$ we can write the partition sum as

$$\begin{aligned} Z &= \prod_q \int d\lambda_q \frac{d\omega_q}{2\pi} \left(\prod_a d\rho_q^a \right) e^{-i\omega_q \lambda_q + i\omega_q \frac{g^4}{q^4} \text{tr} |\rho_q|^2} e^{-\frac{d^2q}{(2\pi)^2} \frac{q^4}{g^4} \frac{\lambda_q}{\mu^2}} \\ &= \left[\prod_q \int d\lambda_q \frac{d\omega_q}{2\pi} e^{-i\omega_q \lambda_q} e^{-\frac{d^2q}{(2\pi)^2} \frac{q^4}{g^4} \frac{\lambda_q}{\mu^2}} \right] \underbrace{\prod_q \int \left(\prod_a d\rho_q^a \right) e^{i\omega_q \frac{g^4}{q^4} \text{tr} |\rho_q|^2}}_{\tilde{Z}[\omega_q]}. \end{aligned} \quad (21)$$

The first line of the equation above is obtained from the original partition sum (18) by inserting a δ -functional

$$1 = \int \prod_q d\lambda_q \delta \left(\lambda_q - \frac{g^4}{q^4} \text{tr} |\rho_q|^2 \right) \quad (22)$$

which fixes $\lambda(q) = (g^4/q^4) \text{tr} |\rho(q)|^2$. To compute $\tilde{Z}(\omega_q)$ we again introduce the constraint field $g^2 \text{tr} |A^+(q)|^2 = X(q)$,

$$\begin{aligned} \tilde{Z}[\omega_q] &= \int \prod_q dX_q \left(\prod_a d\rho_q^a \right) \delta \left(X_q - \frac{g^4}{q^4} \text{tr} |\rho_q|^2 \right) e^{i\omega_q \frac{g^4}{q^4} \text{tr} |\rho_q|^2} \\ &\sim \prod_q \int dX_q X_q^{\frac{N_c^2}{2}} e^{i\omega_q X_q}. \end{aligned} \quad (23)$$

Inserting this into Eq. (21) we obtain

$$\begin{aligned} Z &= \prod_q \int dX_q e^{-\frac{d^2q}{(2\pi)^2} \frac{q^4}{g^4} \frac{X_q}{\mu^2} + \frac{1}{2} N_c^2 \log X_q} \\ &= \int \mathcal{D}X(q) e^{-\int \frac{d^2q}{(2\pi)^2} \left[\frac{q^4}{g^4 \mu^2} X(q) - \frac{1}{2} A_\perp N_c^2 \log X(q) \right]}. \end{aligned} \quad (24)$$

In the last step we have taken the continuum limit, A_\perp is the transverse area covered by the integration over the impact parameter b in Eq. (20). The effective potential for the function $X(q)$ is therefore

$$V_{\text{eff}}[X(q)] = \int \frac{d^2q}{(2\pi)^2} \left[\frac{q^4}{g^4 \mu^2} X(q) - \frac{1}{2} A_\perp N_c^2 \log X(q) \right], \quad (25)$$

and its stationary point corresponds to the average gluon distribution (at order $\sim N_c^2$)

$$\frac{\delta}{\delta X(k)} V_{\text{eff}}[X(q)] = 0 \rightarrow X_s(k) \equiv \langle g^2 \text{tr} |A^+(k)|^2 \rangle = \frac{1}{2} N_c^2 A_\perp \frac{g^4 \mu^2}{k^4}. \quad (26)$$

The contribution to $V_{\text{eff}}[X(q)]$ at zeroth order in N_c can be restored by comparing to $X_s(k)$ obtained directly from the Gaussian two-point function:

$$\langle \rho^a(k) \rho^b(q) \rangle = \delta^{ab} (2\pi)^2 \delta(k+q) \mu^2 \rightarrow X_s(k) = \frac{1}{2} (N_c^2 - 1) A_\perp \frac{g^4 \mu^2}{k^4}. \quad (27)$$

Hence, to restore the $\mathcal{O}(1)$ contribution to $V_{\text{eff}}[X(q)]$ Eq. (25) should be modified to

$$V_{\text{eff}}[X(q)] = \int \frac{d^2q}{(2\pi)^2} \left[\frac{q^4}{g^4\mu^2} X(q) - \frac{1}{2} A_{\perp} (N_c^2 - 1) \log X(q) \right]. \quad (28)$$

We shall mostly focus on Eq. (25) in what follows but refer to (28) when $\mathcal{O}(N_c^0)$ accuracy of the gluon distribution $X(q)$ would be needed.

The two-point correlator $\langle \rho^a(q) \rho^b(k) \rangle$ of the color charge, averaged over *all* of its fluctuations, follows from the action $S[\rho]$ and is written in Eq. (27). In order to explicitly split off the fluctuations of $\rho(q)$ at fixed $X(q)$ we can write this in the form

$$\langle \rho^a(q) \rho^b(k) \rangle = 2 \frac{q^4}{g^4} \frac{1}{N_c^2 A_{\perp}} \delta^{ab} (2\pi)^2 \delta(k+q) \int \mathcal{D}X(q) e^{-V_{\text{eff}}[X]} X(q). \quad (29)$$

Replacing the integration over $X(q)$ by the extremal solution $X_s(q)$ reproduces the correlator from Eq. (27). This last expression should be useful for future applications where one may want to explicitly isolate the fluctuations of the gluon distribution $X(q)$ from more complicated expressions involving two-point functions of $\rho(q)$.

We briefly pause our derivation at this point to comment on the potential describing fluctuations of the Weizsäcker-Williams gluon distribution defined via the light-cone gauge field $A^i(q)$. Because of the non-linear dependence of A^i on ρ we are unable to compute the effective potential analytically except in the weak field regime where $A^i(q) = ig(q^i/q^2)\rho(q)$. Hence, in this regime both the diagonal as well as the off-diagonal components of the WW gluon distribution, $\delta^{ij} \text{tr} A^i(q) A^j(-q)$ and $(2q^i q^j / q^2 - \delta^{ij}) \text{tr} A^i(q) A^j(-q)$, respectively, are equal to $q^2 \text{tr} A^+(q) A^+(-q)$. The effective potential for these distributions is therefore again given by Eq. (25) with the replacement $q^4 \rightarrow q^2$ in the first term of the integrand.

As a second aside we briefly illustrate the modifications due to adding a quartic color charge operator to the quadratic action. We choose a particularly simple form in order to be able to compute the effective potential exactly without having to resort to a perturbative expansion:

$$S_4 = \frac{1}{\beta} \int d^2x d^2y \rho^a(x) \rho^a(x) \rho^b(y) \rho^b(y) = \frac{1}{\beta} \int \frac{d^2q_1}{(2\pi)^2} \frac{d^2q_2}{(2\pi)^2} \rho^a(q_1) \rho^a(-q_1) \rho^b(q_2) \rho^b(-q_2). \quad (30)$$

This replaces eq. (21) by

$$Z = \left[\prod_q \int d\lambda_q \frac{d\omega_q}{2\pi} e^{-i\omega_q \lambda_q} \right] e^{-\frac{d^2q}{(2\pi)^2} \sum_q \frac{q^4}{g^4} \frac{\lambda_q}{\mu^2} - \frac{d^2q}{(2\pi)^2} \frac{d^2q}{(2\pi)^2} \frac{1}{\beta g^4} \sum_{q_1, q_2} q_1^4 q_2^4 \lambda(q_1) \lambda(q_2)} \tilde{Z}[\omega_q] \quad (31)$$

$$= \int \mathcal{D}X(q) e^{-\int \frac{d^2q}{(2\pi)^2} \left[\frac{q^4}{g^4\mu^2} X(q) - \frac{1}{2} A_{\perp} N_c^2 \log X(q) \right] - \frac{1}{\beta g^4} \left(\int \frac{d^2q}{(2\pi)^2} q^4 X(q) \right)^2}. \quad (32)$$

Hence, in this case

$$V_{\text{eff}}[X(q)] = \int \frac{d^2q}{(2\pi)^2} \left[\frac{q^4}{g^4\mu^2} X(q) - \frac{1}{2} A_{\perp} N_c^2 \log X(q) \right] + \frac{1}{\beta g^4} \left(\int \frac{d^2q}{(2\pi)^2} q^4 X(q) \right)^2. \quad (33)$$

In the MV model $\mu^2 \sim g^2 A^{1/3}$, where $A^{1/3}$ denotes the thickness of the nucleus, while the coupling β for the quartic color charge density operator involves two additional powers of $gA^{1/3} \gg 1$ [9]. Such a quartic in ρ operator therefore represents a higher order correction in the high gluon density power counting scheme where $g^4 A^{1/3} = \mathcal{O}(1)$, c.f. next subsection. Moreover, in fig. 5 below we shall show that the exact numerical solution of the LO small- x evolution equation agrees rather well with the effective potential for the gluon distribution derived from a quadratic action. We will therefore neglect S_4 in what follows.

We now return to our discussion of the fluctuations of $X(q) = g^2 \text{tr} |A^+(q)|^2$ in the model with a quadratic action and write

$$X(q) = X_s(q) + \delta X(q) \quad (34)$$

and expand $V_{\text{eff}}[X(q)]$ to quadratic order in $\delta X(q)$. This “one loop” approximation leads to

$$\begin{aligned} \Delta V_{\text{eff}}[\delta X(q)] &\equiv V_{\text{eff}}[X(q)] - V_{\text{eff}}[X_s(q)] \\ &\simeq \frac{1}{2} \int \frac{d^2 l}{(2\pi)^2} \frac{d^2 k}{(2\pi)^2} \delta X(l) \left\{ \frac{\delta}{\delta X(l)} \frac{\delta}{\delta X(k)} V_{\text{eff}}[\delta X(q)] \right\} \delta X(k) \\ &= \frac{1}{2} \int \frac{d^2 q}{(2\pi)^2} \frac{\delta X(q)^2}{X_s(q)^2} \frac{1}{2} N_c^2 A_{\perp} \end{aligned} \quad (35)$$

$$\rightarrow \int \mathcal{D} \delta X(q) e^{-V_{\text{eff}}[\delta X(q)]} = e^{-\frac{1}{2} \text{tr} \log \left(\frac{1}{2} \frac{N_c^2 A_{\perp}}{X_s(q)^2} \right)}. \quad (36)$$

However, it is clear from the form of $V_{\text{eff}}[X(q)]$ that the quadratic approximation can not describe fluctuations far from the extremal solution $X_s(q)$. We therefore follow a different route. We introduce the fluctuation field $\eta(q)$ through

$$X(q) = X_s(q) \eta(q), \quad (37)$$

with $X_s(q)$ as written in Eq. (26). A fluctuation from the extremal “path” $X_s(q)$ has action

$$\begin{aligned} \Delta V_{\text{eff}}[\eta(q)] &\equiv V_{\text{eff}}[\eta(q)] - V_{\text{eff}}[\eta(q) = 1] \\ &= \frac{1}{2} N_c^2 A_{\perp} \int \frac{d^2 q}{(2\pi)^2} [\eta(q) - 1 - \log \eta(q)]. \end{aligned} \quad (38)$$

This is a Liouville action (without kinetic term and with negative Ricci scalar) for the field $\phi(q) = \log \eta(q)$ in two dimensional q -space⁶. Indeed, the canonical dimension of the fluctuation field $\eta(q)$ as introduced in Eq. (37) is zero. This will become important below to understand the spectrum of fluctuations from small- x evolution.

In the following section we use expression (38) to analyze the correlation of gluon number and transverse momentum fluctuations.

A. Parametric dependence on the number of colors and on the thickness of the target

In this subsection we discuss the parametric dependence of the fluctuations on N_c and on the thickness of the target nucleus which is proportional to the third root of its atomic number, $A^{1/3}$. In particular, we outline that the fluctuations of the gluon distribution considered here are of the same order in $A^{1/3}$ as the “extremal” (or average) gluon distribution $X_s(q)$, and of the same or lower order in N_c . As explained by Kovchegov [17], quantum evolution at leading order applies when $\alpha_s \ll 1$ with $\alpha_s^2 A^{1/3} \sim 1$. The latter condition implies that contributions which do not exhibit longitudinal coherence, i.e. those which are not proportional to the thickness of the nucleus, in this power counting scheme formally correspond to higher order corrections.

Recall from the previous section that the average gluon distribution $X_s(q) \sim N_c^2 g^4 \mu^2 \sim N_c^2 \alpha_s^2 A^{1/3}$. The action (25) evaluated at $X_s(q)$ is $V_{\text{eff}}[X_s(q)] \sim N_c^2$ (times a numerical factor equal to zero in dimensional regularization in $D = 2 - \epsilon$ dimensions). This corresponds to the action of classical gluon fields times a factor of g^2 from the coupling to the sources (see Fig. 1).

In order to be able to evolve initial fluctuations to small x using leading order evolution these fluctuations $\delta X(q) \equiv X_s(q) \eta(q)$ must also be of order $A^{1/3}$. This is satisfied since the effective action (38) for the fluctuation field $\eta(q)$ does not involve the thickness $\sim A^{1/3}$ explicitly. Indeed, the MV model [4] outlined in the Introduction describes precisely these longitudinally coherent valence color charge fluctuations. In other words, fluctuations $\delta X(q) \equiv X_s(q) \eta(q)$ corresponding to a penalty action $\Delta V_{\text{eff}}[\eta(q)]$ which is *independent* of $A^{1/3}$ are of the same order in $A^{1/3}$ as the average gluon distribution $X_s(q)$ and can be evolved to small x . However, one can not study fluctuations with a suppression probability p such that $\log p^{-1} = V_{\text{eff}}[\eta(q)] \sim (A^{1/3})^{-1}$ since that would correspond to $\eta(q) = \mathcal{O}((A^{1/3})^{-1})$ and $\delta X(q) = \mathcal{O}((A^{1/3})^0)$. Such fluctuations are of higher order in the coupling [17].

Power counting in N_c proceeds along similar lines. $\Delta V_{\text{eff}}[\eta(q)]$ is explicitly proportional to N_c^2 , so $\eta(q) = \mathcal{O}(N_c^0)$ corresponds to fluctuations $\delta X(q)$ at the same order in N_c as the average gluon distribution $X_s(q)$. These can be

⁶ In Ref. [16] Iancu and McLerran proposed a Liouville action to describe the fluctuations of Q_s in the transverse impact parameter plane (x -space) due to stochastic high-energy evolution; this is unrelated to our discussion of fluctuations in the ensemble of gluon distributions $X(q)$ which occur even at fixed Q_s , as considered here, and exist even in the absence of QCD evolution (MV model).

selected by an external “trigger” probability p such that $\log p^{-1} = V_{\text{eff}}[\eta(q)] \sim N_c^2$. However, it is allowed to select less suppressed fluctuations corresponding to $\log p^{-1} \sim N_c^0$ provided such terms in the effective action are accounted for, c.f. Eq. (28).

V. GLUON MULTIPLICITY AND TRANSVERSE MOMENTUM FLUCTUATIONS

In this section we analyze fluctuations of the semi-hard gluons above the saturation momentum Q_s and up to a maximum momentum scale $Q_{\text{max}} \gg Q_s$. The number of such gluons for a given $X(q) = g^2 \text{tr} |A^+(q)|^2$ is given by

$$N_g[X(q)] = \int \frac{d^2q}{(2\pi)^2} q^2 X(q) = \int \frac{d^2q}{(2\pi)^2} q^2 X_s(q) \eta(q) . \quad (39)$$

The integral extends from $q^2 = Q_s^2$ up to $q^2 = Q_{\text{max}}^2$. As already mentioned above in the linear regime $q^2 g^2 \text{tr} |A^+(q)|^2$ approaches the Weizsäcker-Williams gluon distribution $g^2 \text{tr} |A^i(q)|^2$, so N_g counts the number of Weizsäcker-Williams gluons from Q_s^2 to Q_{max}^2 . We focus first on the MV model with $\mu^2 = \text{const}$; analogous results for a q -dependent $\mu^2(q)$ shall be summarized at the end of this section.

The number of additional gluons due to the fluctuation about the extremal gluon distribution is given by

$$\Delta N_g[\eta(q)] = \int \frac{d^2q}{(2\pi)^2} q^2 X_s(q) [\eta(q) - 1] . \quad (40)$$

This quantity does not depend on the UV cutoff Q_{max}^2 because the fluctuation has finite support in order to have a finite action.

The average (squared) transverse momentum of gluons between $q^2 = Q_s^2$ and $q^2 = Q_{\text{max}}^2$ can be defined through (see analogous discussion in Ref. [18])

$$\overline{q^2}[X(q)] = \frac{\int \frac{d^2q}{(2\pi)^2} q^2 X(q)}{\int \frac{d^2q}{(2\pi)^2} X(q)} = \frac{N_g[X(q)]}{\int \frac{d^2q}{(2\pi)^2} X(q)} . \quad (41)$$

Here $\overline{q^2}$ refers to an average over the transverse momentum distribution for a given gluon distribution $X(q)$ but *not* to an average over all configurations of A^+ . Once again we subtract the value at the saddle point,

$$\Delta \overline{q^2}[\eta(q)] = \frac{\Delta N_g[\eta(q)]}{\int \frac{d^2q}{(2\pi)^2} X_s(q) \eta(q)} . \quad (42)$$

We now proceed to discuss the effect of fluctuations, $\eta(q) \neq 1$. Our strategy is to introduce a trial function for $\eta(q)$ for which we then evaluate N_g , $\overline{q^2}$, and the “penalty action” ΔS via Eq. (38). Consider the *ansatz*

$$\eta(q) = 1 + \eta_0 \left(\frac{g^4 \mu^2}{q^2} \right)^a \Theta(q^2 - \Lambda^2) \Theta(Q^2 - q^2) . \quad (43)$$

Thus, the fluctuation has support on the interval $\Lambda^2 < q^2 < Q^2$ within the window $Q_s^2 < q^2 < Q_{\text{max}}^2$, i.e. $\Lambda^2 \geq Q_s^2$, $Q^2 \leq Q_{\text{max}}^2$ with $\Lambda^2 \ll Q^2$. Also, by dimensional analysis the multiplicative fluctuation can depend only on q^2/μ^2 since μ^2 is the only dimensionful scale in the MV action (2). We recall from our discussion in sec. IV A that, parametrically,

$$\eta_0 \sim \frac{1}{N_c^2 (g^4 \mu^2)^a} \Delta S , \quad (44)$$

so that for $\Delta S \sim N_c^2$, $\delta X(q) = X_s(q) \eta(q)$ is of the same order in N_c and $A^{1/3}$ as the average gluon distribution $X_s(q)$.

For a fluctuation of the form (43) the excess gluon multiplicity is given by

$$\Delta N_g \simeq \frac{1}{8\pi} N_c^2 A_{\perp} g^4 \mu^2 \eta_0 \times \begin{cases} \frac{1}{a} \left(\frac{g^4 \mu^2}{\Lambda^2} \right)^a & (a > 0) , \\ \log \frac{Q^2}{\Lambda^2} & (a = 0) , \\ \frac{1}{|a|} \left(\frac{Q^2}{g^4 \mu^2} \right)^{|a|} & (a < 0) . \end{cases} \quad (45)$$

The excess (squared) transverse momentum of gluons with transverse momentum above the saturation scale is given by

$$\Delta\bar{q}^2 \simeq Q_s^2 \eta_0 \times \begin{cases} \frac{1}{a} \left(\frac{g^4 \mu^2}{\Lambda^2} \right)^a & (a > 0), \\ \log \frac{Q^2}{\Lambda^2} & (a = 0), \\ \frac{1}{|a|} \left(\frac{Q^2}{g^4 \mu^2} \right)^{|a|} & (a < 0), \end{cases} \quad (46)$$

or

$$\Delta N_g \simeq N_c A_\perp \Delta\bar{q}^2. \quad (47)$$

We have simplified the expression by linearizing in the fluctuation amplitude. The factor of N_c in this equation arises due to the fact that we only integrate over gluons with $q^2 > Q_s^2$ with $Q_s^2 \sim N_c g^4 \mu^2$. According to Eq. (47) the average squared transverse momentum due to the fluctuation is proportional to the excess number of gluons it contains. In the next section we shall confirm such a tight nearly linear correlation of ΔN_g and $\Delta\bar{q}^2$ via Monte-Carlo simulations.

Finally, the penalty action for such a fluctuation $\eta(q)$ is

$$\Delta S[\eta(q)] \simeq \frac{1}{8\pi} N_c^2 A_\perp g^4 \mu^2 \eta_0 \times \begin{cases} \frac{1}{1-a} \left(\frac{Q^2}{g^4 \mu^2} \right)^{1-a} & (a < 1), \\ \log \frac{Q^2}{\Lambda^2} & (a = 1), \\ \frac{1}{a-1} \left(\frac{g^4 \mu^2}{\Lambda^2} \right)^{a-1} & (a > 1). \end{cases} \quad (48)$$

The goal now is to pay as low a price $\Delta S[\eta(q)]$ as possible while maximizing ΔN_g and $\Delta\bar{q}^2$. Fluctuations with $a < 0$, corresponding to increasing $\eta(q)$, come with a large penalty ΔS . In fact, even a flat $\eta(q)$ with $a \rightarrow 0$ corresponds to $\Delta S \sim Q^2$ while, at the same time, ΔN_g and $\Delta\bar{q}^2$ increase only logarithmically with Q^2 . Similarly, fluctuations with $a > 1$, which drop off very rapidly with q^2 , give small ΔS , but also a small multiplicity excess ΔN_g . Therefore, we expect that in the MV model the dominant ‘‘high multiplicity’’ fluctuations would have a high- q tail corresponding to $1 > a > 0$.

We now turn to a q -dependent $\mu^2(q)$ as written in Eq. (8). This corresponds to the non-local Gaussian approximation to the JIMWLK action at small x proposed in Ref. [5] which accounts for the small- x anomalous dimension. Here, the gluon excess above Q_s^2 is

$$\Delta N_g[\eta(q)] \simeq \frac{1}{8\pi} N_c^2 A_\perp g^4 \mu_0^2 \frac{\eta_0}{1 - \gamma - a} \left(\frac{Q^2}{Q_s^2} \right)^{1-\gamma} \left(\frac{g^4 \mu_0^2}{Q^2} \right)^a, \quad (1 - \gamma > a) \quad (49)$$

while the additional transverse momentum contributed by the fluctuation is

$$\Delta\bar{q}^2[\eta(q)] \simeq Q_s^2 \frac{\eta_0}{1 - \gamma - a} \left(\frac{Q^2}{Q_s^2} \right)^{1-\gamma} \left(\frac{g^4 \mu_0^2}{Q^2} \right)^a \quad (-\gamma < a < 1 - \gamma). \quad (50)$$

Once again we have linearized this expression in η_0 . In this approximation the proportionality (47) of ΔN_g and $\Delta\bar{q}^2$ still holds.

The ‘‘penalty’’ action for a fluctuation $\eta(q) \neq 1$ is again given by Eq. (48) with $\mu^2 \rightarrow \mu_0^2$. Contrary to the MV model, near scale invariant fluctuations with $a \approx 0$ may now be significant. While they do come with a ‘‘penalty’’ proportional to Q^2 ($\Delta S \sim \eta_0 N_c^2 A_\perp Q^2$) they also increase substantially the gluon number ΔN_g and the transverse momentum $\Delta\bar{q}^2$ by a power rather than a logarithm of Q^2 .

VI. MONTE-CARLO SIMULATIONS

In this section we show results of numerical Monte-Carlo simulations. The technical aspects of these Monte-Carlo simulations are standard by now, our specific implementation has been discussed in some detail in Ref. [12]. We generate random color charge configurations according to the MV model action; for each configuration we have computed the number of gluons N_g as well as their average (squared) transverse momentum \bar{q}^2 as described in the previous section. These quantities have been integrated up to the lattice cutoff at about $Q \sim 85Q_s$ (for $Y = 0$) resp. $Q \sim 35Q_s$ (for $\alpha_s Y = 1$). We should stress that these initial configurations have been generated with a uniform μ^2

across the transverse impact parameter plane. Hence, there are no “voids” in the target nor is there a boundary to vacuum.

We have also solved the leading order B-JIMWLK renormalization group equation [19, 20] at fixed coupling to a rapidity $Y = 1/\alpha_s$ and performed a similar analysis on those configurations. JIMWLK evolves each Wilson line $V(x_\perp)$ from rapidity 0 to Y where we take

$$X(q) = \int d^2b \int d^2r e^{-iqr} \text{tr} \left[V_Y \left(b - \frac{r}{2} \right) V_Y^\dagger \left(b + \frac{r}{2} \right) - 1 \right]. \quad (51)$$

The saturation scale $Q_s(Y)$ is determined implicitly from the dipole forward scattering amplitude introduced in Eq. (4) above: $\mathcal{N}_Y(r = \sqrt{2}/Q_s) = 1 - 1/\sqrt{e}$. Note that $\mathcal{N}_Y(r)$ is averaged over all configurations.

The gluon distribution at a fixed impact parameter b is given by the Wigner distribution

$$X_W(q, b) \equiv \frac{dX(q)}{d^2b} = \int d^2r e^{-iqr} \text{tr} \left[V_Y \left(b - \frac{r}{2} \right) V_Y^\dagger \left(b + \frac{r}{2} \right) - 1 \right]. \quad (52)$$

$X_W(q, b)$ is neither real (for $N_c \geq 3$ colors) nor positive definite since gluons can not be localized both in transverse momentum and impact parameter space. The Wigner distribution has to be averaged over transverse area patches of linear dimension $\gtrsim 1/Q_s$ to be interpreted as the distribution of gluons with transverse momenta $q \geq Q_s$.

Computationally instead it is much more efficient to analyze

$$X_R(q, b) = \int d^2x \int d^2y e^{-iq(y-x)} e^{-\frac{(b-x)^2}{2R^2}} e^{-\frac{(b-y)^2}{2R^2}} \text{tr} \left[V_Y(x) V_Y^\dagger(y) - 1 \right], \quad (53)$$

which is similar to the smeared Wigner distribution of hard gluons. It corresponds to the gluon distribution at impact parameter b averaged over distance scales of order R . The limit $R \rightarrow \infty$ takes $X_R(q, b)$ back to $X(q)$. The numerical results presented below were obtained using $R = 2/Q_s(Y)$.

The B-JIMWLK equations describe fluctuations only up to scales where the dipole scattering amplitude drops to $\mathcal{O}(\alpha_s^2)$, see the review [21] and references therein. At such scales the fact that the number of gluons in the hadron is discrete leads to large fluctuations in the evolution speed [22]. However, the running of the coupling in QCD delays the effects of these fluctuations (related to the discrete number of gluons) to very high rapidities [23]. Hence, for rapidities and transverse momenta of practical interest the JIMWLK equations may be a useful approximation, at least for those regions in impact parameter space where the gluon density is not too low.

We now present the results obtained from the Monte-Carlo simulation. In Fig. 2 we show the correlation of $\Delta\bar{q}^2$

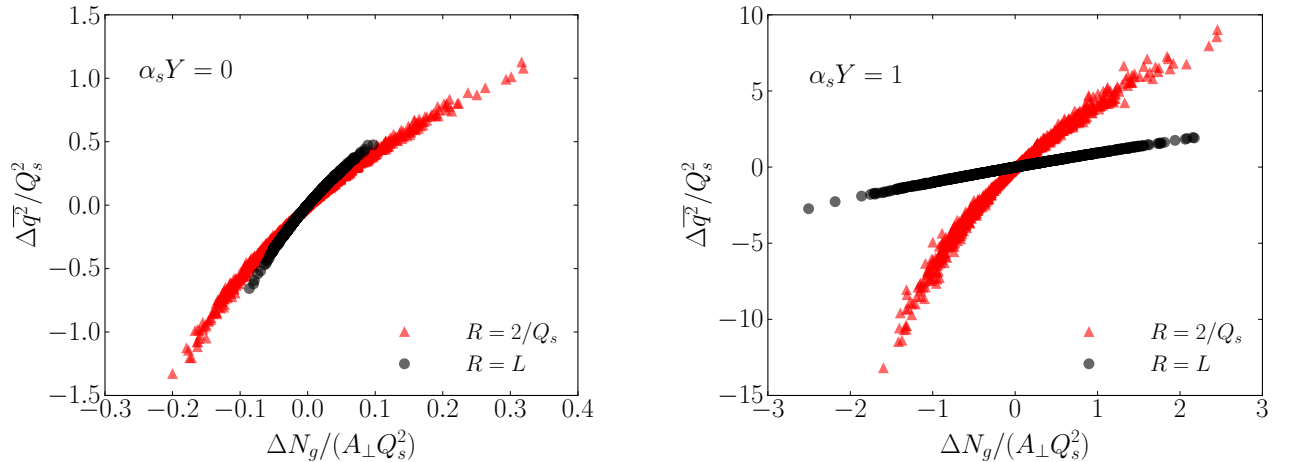


FIG. 2: Fluctuations of the gluon density and average squared transverse momentum in a random Monte-Carlo sample of 150 configurations of the small- x fields. The gluon distribution has either been averaged over a Gaussian of width $R = 2/Q_s(Y)$ centered at a random impact parameter or over the entire 2d impact parameter plane of a large lattice ($L \simeq 18/Q_s(Y = 0)$). The transverse area is taken as $A_\perp = 2\pi R^2$ or $A_\perp = L^2$, respectively. A bar refers to an average over all gluons with transverse momentum $q > Q_s(Y)$ for a given configuration. Left: evolution rapidity $Y = 0$ corresponds to the MV model. Right: the fields have been evolved to $Y = 1/\alpha_s$ via the JIMWLK equations.

and ΔN_g . The MC data shows a tight positive correlation of the transverse momentum vs. gluon density fluctuation,

as expected. The magnitude of the fluctuations of both the gluon density per unit transverse area $\Delta N_g/A_\perp$ as well as of the typical squared transverse momentum $\Delta \bar{q}^2$ has increased by essentially an order of magnitude from $Y = 0$ to $Y = 1/\alpha_s$; this is despite the fact that both axes in Fig. 2 have been scaled by $1/Q_s^2(Y)$ to make them dimensionless. It is also interesting to see that in the MV model the fluctuations essentially scale with “volume”, i.e. ΔN_g is approximately proportional to A_\perp while $\Delta \bar{q}^2$ is independent of A_\perp . At $Y = 1/\alpha_s$ on the other hand, the solution of JIMWLK clearly exhibits finite range correlations since averaging over a large “volume” strongly reduces $\Delta \bar{q}^2$ at fixed density $\Delta N_g/A_\perp$.

It is interesting to obtain a rough idea of the magnitude of ΔN_g for reasonable values of A_\perp and $Q_s(Y)$. A semi-hard process may effectively average the target gluon fields over an area of order $A_\perp \simeq 0.1 \text{ fm}^2$. Choosing a target saturation momentum of $Q_s(Y) = 1 \text{ GeV}$ we can then translate $\Delta N_g/(A_\perp Q_s^2) = 1, 2, 3$ on the horizontal axis of Fig. 2 to $\Delta N_g \simeq 5, 10, 15$ additional semi-hard gluons; for $Q_s(Y) \simeq 2.5 \text{ GeV}$ this increases to about $\Delta N_g \simeq 30, 60, 90$ excess gluons in the target.

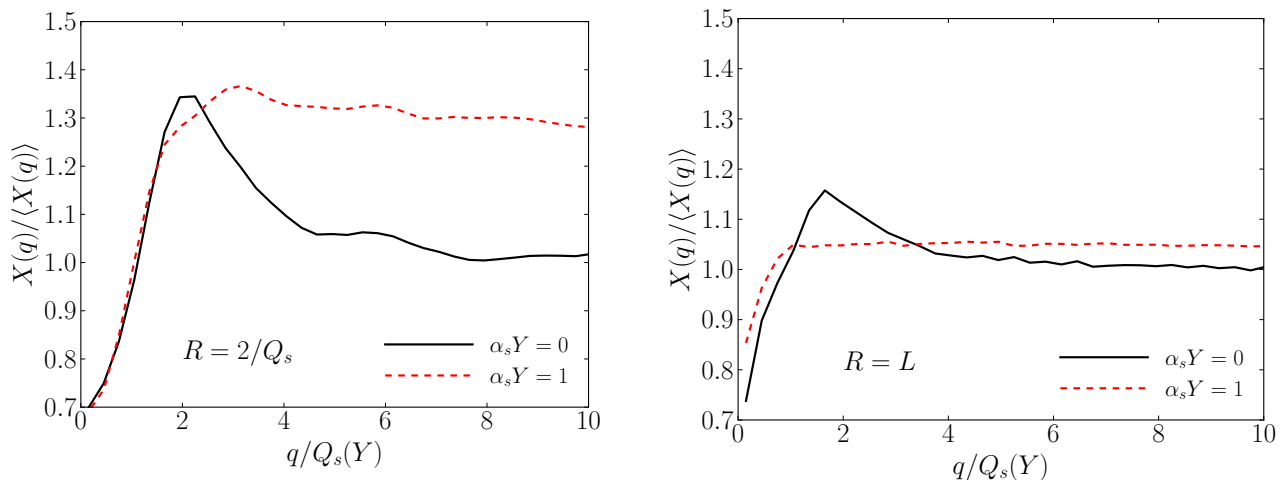


FIG. 3: Fluctuation of the gluon distribution $X(q) = g^2 \text{tr} |A^+(q)|^2$ in the MV model ($Y = 0$, solid line) and after leading order, fixed coupling JIMWLK evolution to $\alpha_s Y = 1$ (dashed line). The left panel corresponds to the gluon distribution integrated over a Gaussian of width $R = 2/Q_s(Y)$ centered at a random impact parameter; for the panel on the right the gluon distribution has been integrated over the entire 2d impact parameter plane of a large lattice ($L \simeq 18/Q_s(Y = 0)$). To obtain smooth curves we have averaged over a subsample of 100 configurations (out of 1000 total) with the highest gluon multiplicity N_g .

The spectral shape of high-multiplicity fluctuations is shown in Fig. 3. For the MV model the dominant fluctuations contain additional gluons with transverse momenta up to a few times Q_s , then drop off smoothly to unity for $q \gg Q_s$. Qualitatively, this tail corresponds to our *ansatz* (43) with $a > 0$. At high rapidity quantum fluctuations change the shape of fluctuations to a flat, essentially scale independent distribution, so $a \approx 0$ in Eq. (43). The different q -dependence of the fluctuations illustrates the different role of the saturation scale Q_s in the MV model vs. JIMWLK evolution: in the MV model this scale truly affects the dynamics of fluctuations which “pile up” just above Q_s . If the hadronic wave function evolves to much smaller x , on the other hand, Q_s is not a prominent scale in the fluctuation spectrum but acts merely as an absorptive boundary for BFKL emissions [7]. Indeed, recall that the canonical dimension of $\eta(q)$ is zero and that the JIMWLK evolution kernel at fixed coupling is scale invariant.

Fig. 3 also shows that as expected fluctuations in a smaller “volume” have greater amplitude. Other than that the spectral shape of $\eta(q)$ averaged over small ($R = 2/Q_s(Y)$) or large scales in the impact parameter plane is similar.

Amusingly, Fig. 3 resembles qualitatively the “disappearance of the Cronin peak” due to small- x evolution [24]. Of course, the latter refers to the *averaged* evolution of the *ratio* of the gluon distributions of a dense to a dilute target. In contrast, Fig. 3 shows the transverse momentum spectrum of fluctuations of the gluon distribution of a single target about the average/extremal function.

Configurations with *lower* than average gluon multiplicity exhibit fluctuations with a similar spectral shape as high multiplicity configurations as shown in Fig. 4. In the MV model there is a dip in the gluon distribution just above the saturation momentum, and the gluon distribution then smoothly approaches the average distribution at higher q . On the other hand, JIMWLK evolution again generates a scale invariant fluctuation and a uniform depletion of gluons for transverse momenta greater than (one or two times) $Q_s(Y)$.

We have also checked that the fluctuations of the gluon distribution are indeed described by the Liouville potential (up to a field redefinition) derived above in Eq. (38). In the MC simulation this can be achieved by recording a

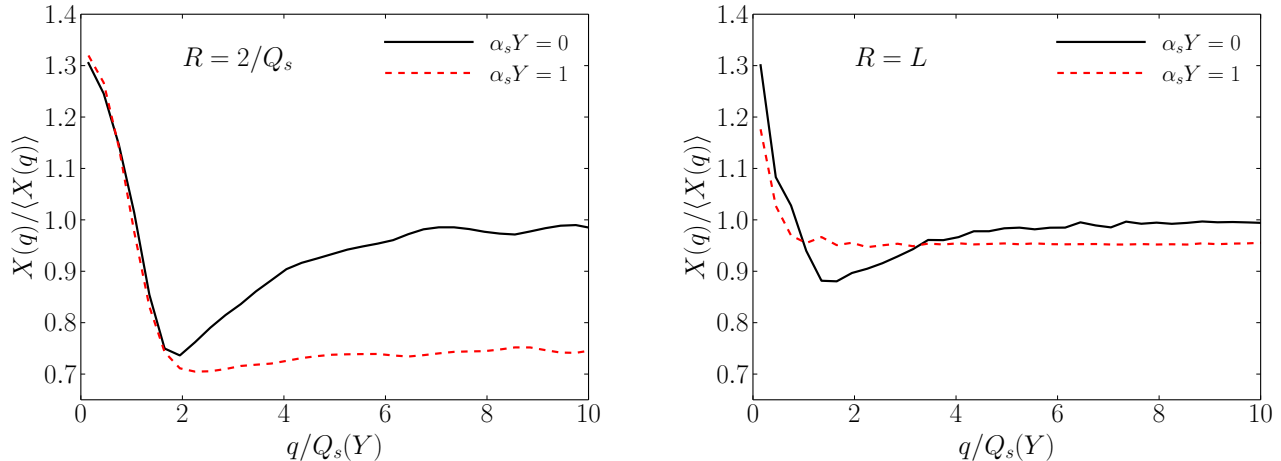


FIG. 4: Spectral shape of low gluon multiplicity configurations. See Fig. 3 for further details.

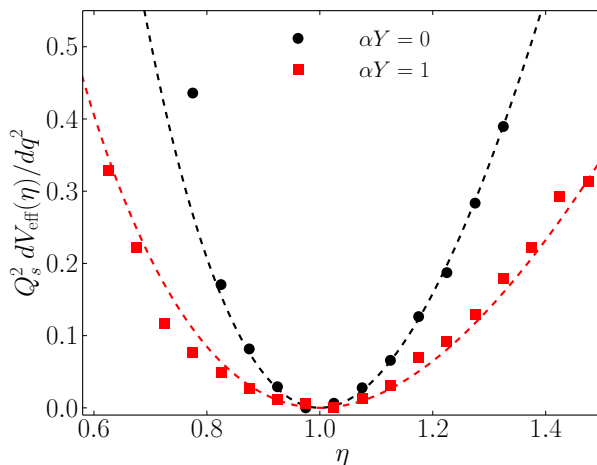


FIG. 5: The effective potential describing fluctuations of the covariant gauge gluon distribution (beyond the saturation scale) in a transverse area patch of order $2\pi R^2 = 8\pi/Q_s^2(Y)$. Symbols show the results obtained from the MC simulation, lines correspond to the potential derived analytically (see text).

histogram of $\eta(q) = X_R(q, b)/\langle X_R(q, b) \rangle$ in the vicinity of an arbitrary impact parameter. See appendix A for details. We compare the simulation results to

$$\frac{dV_{\text{eff}}}{dq^2} = \frac{1}{8\pi} N_c^2 A_{\perp} [\eta - 1 - \log \eta] . \quad (54)$$

The gluon distribution $X_R(q, b)$ has been “smeared out” over a Gaussian of area $2\pi R^2$ centered at impact parameter b as described above. Nevertheless, the quantity A_{\perp} in Eq. (54) is a *dynamical* scale corresponding to the transverse area occupied by the fluctuations $\eta(q)$ of the gluon distribution. In particular, A_{\perp} may very well be less than $2\pi R^2$ if fluctuations occur over shorter length scales.

In Fig. 5 we compare the numerical results to Eq. (54); A_{\perp} in that equation has been treated as a free parameter adjusted to best fit the MC data⁷. Most significantly we observe that the linear minus logarithmic potential from Eq. (54) indeed does describe the simulation results rather well (within statistical uncertainties).

⁷ The simulation is carried out for $N_c = 3$ colors while Eq. (54) applies in the large- N_c limit. Subleading corrections simply rescale A_{\perp} . With the prefactor from Eq. (54) the best fits correspond to $A_{\perp} Q_s^2 \simeq 23.75$ at $Y = 0$, which is close to the geometric area $2\pi R^2 Q_s^2 = 8\pi$; and $A_{\perp} Q_s^2 = 10.22$ at rapidity $\alpha_s Y = 1$.

VII. DISCUSSION AND OUTLOOK

In this paper we have described a new attempt at understanding fluctuations of a physical observable $O[A^+]$, for example of the (covariant gauge) gluon distribution $O[A^+] = g^2 \text{tr} |A^+(q)|^2$, induced by fluctuations of the classical small- x color fields. Of course, fluctuations of the multiplicity in small- x evolution have been studied before, see for example the recent paper [25] and references therein. These are typically formulated in terms of dipole splitting processes. Instead, our approach here involves the small- x effective action $S[A^+]$, resp. the weight functional $W[A^+]$. We stress that here A^+ refers to the soft *classical* field generated by integrating out hard partons [4, 20] and representing them by random valence charge sources. The semi-classical treatment of fluctuations requires that one selects fluctuations which are suppressed by a probability p which is independent of the thickness $\sim A^{1/3}$ of the target nucleus. The resulting fluctuation of the two-point function of A^+ is then proportional to the thickness, just like the extremal gluon distribution itself. That is, such fluctuations of the small- x field are induced by longitudinally coherent fluctuations of the valence charges as described (at moderately small x) by the MV model, and as re-summed by JIMWLK evolution. In contrast, the treatment of fluctuations corresponding to a suppression factor $p \sim \exp(-1/A^{1/3})$ require higher-order corrections in the coupling [17].

Our approach allows us to discuss fluctuations even in the absence of strong small- x evolution, e.g. in the McLerran-Venugopalan model. Furthermore, it can be applied to observables which may be more difficult to access in dipole splitting approaches. For example, we can define, and in principle compute, the functional distribution of the Weizsäcker-Williams gluon distribution:

$$e^{-V_{\text{eff}}[X(q)]} = \int \mathcal{D}\rho(q) W[\rho(q)] \delta(X(q) - g^2 \text{tr} |A^i(q)|^2). \quad (55)$$

We have computed this potential analytically in the weak field limit ($A^i \sim 1$), and for a large number of colors ($N_c \gg 1$). Nevertheless, it is feasible, in principle, to compute it from Eq. (55) even when $gA^i \sim 1$ and for any N_c , perhaps numerically. At next to leading order in the field strength, for example, we have in terms of the covariant gauge field

$$\begin{aligned} \delta^{ij} g^2 \text{tr} A^i(q) A^j(-q) &= \frac{1}{2} q^2 g^2 A^{+a}(q) A^{+a}(-q) \\ &\quad - \frac{g^4}{8} f^{abe} f^{cde} \left(\delta^{lm} - \frac{q^l q^m}{q^2} \right) \int \frac{d^2 k}{(2\pi)^2} \frac{d^2 p}{(2\pi)^2} k^l p^m A^{+a}(q-k) A^{+b}(k) A^{+c}(-q-p) A^{+d}(p) \end{aligned} \quad (56)$$

$$\begin{aligned} \left(2 \frac{q^i q^j}{q^2} - \delta^{ij} \right) g^2 \text{tr} A^i(q) A^j(-q) &= \frac{1}{2} q^2 g^2 A^{+a}(q) A^{+a}(-q) \\ &\quad + \frac{g^4}{8} f^{abe} f^{cde} \left(\delta^{lm} - \frac{q^l q^m}{q^2} \right) \int \frac{d^2 k}{(2\pi)^2} \frac{d^2 p}{(2\pi)^2} k^l p^m A^{+a}(q-k) A^{+b}(k) A^{+c}(-q-p) A^{+d}(p) \end{aligned} \quad (57)$$

The first line is the conventional Weizsäcker-Williams gluon distribution, the second line is the so-called distribution of linearly polarized gluons⁸. The fluctuations of these distributions can be determined by substituting the r.h.s. of Eqs. (56,57) into the delta-functional in Eq. (55). An explicit analytic calculation at next to leading order in gA^+ is complicated by the fact that the corrections are non-local in transverse momentum space. We leave this computation for future work.

As an application of interest to us we have used our approach to determine the fluctuations of the (covariant gauge) gluon distribution $g^2 \text{tr} |A^+(q)|^2$. This allowed us to study the correlation of the fluctuations of the number of gluons (above the saturation scale) and of their typical transverse momentum squared⁹. We find that these quantities are very tightly correlated so that an increase (decrease) in the gluon density per unit transverse area corresponds to an upward (downward) fluctuation of the squared transverse momentum. The solution of the JIMWLK small- x RG exhibits a much stronger increase of $\Delta \bar{q}^2$ with the gluon density $\Delta N_g/A_\perp$ in small ‘‘volumes’’ (transverse patches of size a few times $1/Q_s^2(Y)$), presumably due to the presence of finite range correlations in the impact parameter plane.

The shape of such high-multiplicity fluctuations in transverse momentum space is modified significantly by JIMWLK evolution to small x as compared to the MV model. The latter adds hard gluons mainly right above the saturation

⁸ For an introduction into these gluon distributions see, for example, Ref. [26]. Their expectation values, i.e. their values at the extremum of V_{eff} , have been computed to all orders in gA^+ within the MV model [27] as well as at small x [28]. Expectation values of other such ‘‘transverse momentum dependent’’ (TMD) gluon distributions at small x have been computed in Ref. [29].

⁹ We stress that we consider the number or transverse momentum of gluons in a single hadron or nucleus and not multiplicity or transverse momentum fluctuations in a collision of two hadrons or nuclei. The latter has been investigated, for example, in Refs. [30].

scale. On the other hand, the solution of the small- x renormalization group (in the JIMWLK approximation) gives approximately scale independent multiplicative fluctuations. In other words, the fluctuations that emerge in the small- x limit are better characterized as scale invariant fluctuations of a dimensionless field which multiplies the average gluon distribution, rather than as fluctuations of the absorptive boundary [7] set by the saturation momentum. A nearly scale invariant spectral distribution of high (or low) multiplicity fluctuations are a clear signature for perturbative quantum evolution with a conformal evolution kernel. It would be interesting to check the modification of the fluctuation spectrum due either to a running coupling or at full NLO level.

Appendix A: Obtaining the effective potential from numerical MC simulations

In this appendix we present more details on how the effective potential presented in Fig. 5 has been extracted from the numerical simulation.

At a given rapidity, Y , for a given configuration of Wilson lines $V_Y(x_\perp)$, we compute the observable $X_R(q, b = 0)$ using Eq. (53) on a square $N \times N$ lattice in q -space. Next, we split $X_R(q)$ into bins of q^2 defined by

$$q^2 = \frac{4}{a^2} \sum_{n=1,2} \sin^2 \frac{\pi i_n}{N}, \quad (\text{A1})$$

where i_n denotes the lattice site in the n -direction and a is the lattice spacing. We then compute the ratio $\eta(q^2) = X_R(q^2)/\langle X_R(q^2) \rangle$ for each configuration in each momentum bin. In each bin of q^2 we again construct a histogram of the distribution of values of $\eta(q^2)$ as it fluctuates configuration by configuration. This results in a two-dimensional histogram of the number of counts C as a function of η and q^2 . The logarithm of the number of counts, modulo an additive constant $\log \mathcal{N}$, is the differential effective potential with negative sign, i.e.

$$\frac{dV_{\text{eff}}}{dq^2} = -\log(\mathcal{N}C(\eta, q^2)) . \quad (\text{A2})$$

The constant \mathcal{N} is chosen such that $\frac{dV_{\text{eff}}}{dq^2} = 0$ at $\eta = 1$. We have checked that within numerical uncertainties this shift of the potential is about the same in each momentum bin within the range $4 < q^2/Q_s^2 < 50$. We have also found that in this range $\frac{dV_{\text{eff}}}{dq^2}$ is momentum independent, within statistical uncertainties. This enabled us to average over all momenta in this range. The resulting potential is presented in Fig. 5.

Acknowledgements

We thank Yu. Kovchegov, A. Kovner, A. Mueller, and R. Venugopalan for useful comments at the RBRC Workshop ‘‘Saturation: Recent Developments, New Ideas and Measurements’’; April 26-28, 2017, Brookhaven National Laboratory.

A.D. gratefully acknowledges support by the DOE Office of Nuclear Physics through Grant No. DE-FG02-09ER41620; and from The City University of New York through the PSC-CUNY Research grant 69362-0047.

-
- [1] L. V. Gribov, E. M. Levin and M. G. Ryskin, Phys. Rept. **100**, 1 (1983);
Yu. V. Kovchegov, E. Levin: ‘‘Quantum Chromodynamics at High Energy’’, Cambridge Monographs, Cambridge Univ. Press (2012)
 - [2] H. Weigert, Prog. Part. Nucl. Phys. **55**, 461 (2005).
 - [3] A. Kovner, Acta Phys. Polon. B **36**, 3551 (2005).
 - [4] L. D. McLerran and R. Venugopalan, Phys. Rev. D **49**, 2233 (1994); Phys. Rev. D **49**, 3352 (1994);
Y. V. Kovchegov, Phys. Rev. D **54**, 5463 (1996).
 - [5] E. Iancu, K. Itakura and L. McLerran, Nucl. Phys. A **724**, 181 (2003).
 - [6] L. N. Lipatov, Sov. J. Nucl. Phys. **23**, 338 (1976) [Yad. Fiz. **23**, 642 (1976)];
E. A. Kuraev, L. N. Lipatov and V. S. Fadin, Sov. Phys. JETP **45**, 199 (1977) [Zh. Eksp. Teor. Fiz. **72**, 377 (1977)];
I. I. Balitsky and L. N. Lipatov, Sov. J. Nucl. Phys. **28**, 822 (1978) [Yad. Fiz. **28**, 1597 (1978)].
 - [7] A. H. Mueller and D. N. Triantafyllopoulos, Nucl. Phys. B **640**, 331 (2002).
 - [8] S. Jeon and R. Venugopalan, Phys. Rev. D **70**, 105012 (2004); Phys. Rev. D **71**, 125003 (2005).
 - [9] A. Dumitru, J. Jalilian-Marian and E. Petreska, Phys. Rev. D **84**, 014018 (2011);
A. Dumitru and E. Petreska, Nucl. Phys. A **879**, 59 (2012).

- [10] F. Gelis, T. Lappi and L. McLerran, Nucl. Phys. A **828**, 149 (2009);
B. Schenke, P. Tribedy and R. Venugopalan, Phys. Rev. C **86**, 034908 (2012).
- [11] T. Lappi, A. Dumitru and Y. Nara, Nucl. Phys. A **931**, 354 (2014); Phys. Lett. B **734**, 7 (2014).
- [12] A. Dumitru and V. Skokov, Phys. Rev. D **91**, no. 7, 074006 (2015).
- [13] T. Lappi, A. Ramnath, K. Rummukainen and H. Weigert, Phys. Rev. D **94**, no. 5, 054014 (2016).
- [14] A. Kovner and M. Lublinsky, Phys. Rev. D **92**, no. 3, 034016 (2015) doi:10.1103/PhysRevD.92.034016 [arXiv:1506.05394 [hep-ph]].
- [15] A. Dumitru, J. Lenaghan and R. D. Pisarski, Phys. Rev. D **71**, 074004 (2005);
for earlier work on the constraint effective potential in the quantum theory see L. O’Raifeartaigh, A. Wipf and H. Yoneyama, Nucl. Phys. B **271**, 653 (1986);
C. P. Korthals Altes, Nucl. Phys. B **420**, 637 (1994).
- [16] E. Iancu and L. McLerran, Nucl. Phys. A **793**, 96 (2007).
- [17] Y. V. Kovchegov, Phys. Rev. D **61**, 074018 (2000).
- [18] R. Baier, Y. L. Dokshitzer, A. H. Mueller, S. Peigne and D. Schiff, Nucl. Phys. B **484**, 265 (1997).
- [19] I. Balitsky, Nucl. Phys. B **463**, 99 (1996); Phys. Lett. B **518**, 235 (2001).
- [20] J. Jalilian-Marian, A. Kovner, A. Leonidov and H. Weigert, Nucl. Phys. B **504**, 415 (1997); Phys. Rev. D **59**, 014014 (1998); Phys. Rev. D **59**, 034007 (1999) [Erratum-ibid. D **59**, 099903 (1999)];
J. Jalilian-Marian, A. Kovner and H. Weigert, Phys. Rev. D **59**, 014015 (1998);
E. Iancu, A. Leonidov and L. D. McLerran, Nucl. Phys. A **692**, 583 (2001);
E. Iancu and L. D. McLerran, Phys. Lett. B **510**, 145 (2001);
E. Iancu, A. Leonidov and L. D. McLerran, Phys. Lett. B **510**, 133 (2001);
A. H. Mueller, Phys. Lett. B **523**, 243 (2001);
E. Ferreira, E. Iancu, A. Leonidov and L. McLerran, Nucl. Phys. A **703**, 489 (2002);
H. Weigert, Nucl. Phys. A **703**, 823 (2002);
J. P. Blaizot, E. Iancu and H. Weigert, Nucl. Phys. A **713**, 441 (2003);
A. Kovner and M. Lublinsky, JHEP **0503**, 001 (2005).
- [21] A. H. Mueller, hep-ph/0501012.
- [22] Y. Hatta, E. Iancu, C. Marquet, G. Soyez and D. N. Triantafyllopoulos, Nucl. Phys. A **773**, 95 (2006).
- [23] A. Dumitru, E. Iancu, L. Portugal, G. Soyez and D. N. Triantafyllopoulos, JHEP **0708**, 062 (2007).
- [24] J. L. Albacete, N. Armesto, A. Kovner, C. A. Salgado and U. A. Wiedemann, Phys. Rev. Lett. **92**, 082001 (2004);
D. Kharzeev, Y. V. Kovchegov and K. Tuchin, Phys. Rev. D **68**, 094013 (2003).
- [25] T. Liou, A. H. Mueller and S. Munier, Phys. Rev. D **95**, no. 1, 014001 (2017).
- [26] D. Boer, Few Body Syst. **58**, no. 2, 32 (2017).
- [27] A. Metz and J. Zhou, Phys. Rev. D **84**, 051503 (2011).
- [28] A. Dumitru, T. Lappi and V. Skokov, Phys. Rev. Lett. **115**, no. 25, 252301 (2015).
- [29] C. Marquet, E. Petreska and C. Roiesnel, JHEP **1610**, 065 (2016).
- [30] C. Flensburg, G. Gustafson and L. Lönnblad, JHEP **1108**, 103 (2011);
B. Schenke, P. Tribedy and R. Venugopalan, Phys. Rev. C **89**, no. 2, 024901 (2014).